Original Article

The Role of Fabricated Coral Shell Powder in the Healing of Mandibular Bone Gap in Dogs

Ali Ghazi Atiyah[1], **Layth Mahmoud Alkattan**[2*]

1. Department of Surgery and Obstetrics, College of Veterinary Medicine, University of Tikrit, Tikrit, Iraq.
2. Department of Surgery and Theriogenology, College of Veterinary Medicine, University of Mosul, Mosul, Iraq.

Use your device to scan and read the article online

How to Cite This Article Atiyah, A. Gh., & Alkattan, L. M. (2024). The Role of Fabricated Coral Shell Powder in the Healing of Mandibular Bone Gap in Dogs. *Iranian Journal of Veterinary Medicine, 18*(4), 489-500. http://dx.doi.org/10.32598/ijvm.18.4.1005417

http://dx.doi.org/10.32598/ijvm.18.4.1005417

ABSTRACT

Background: The reconstruction of mandibular bone defects poses a real challenge and difficulty for surgeons; biomaterial bone substitutes are the most used material for reconstructing mandibular bone defects.

Objectives: This study explored the role of fabricated hydroxyapatite (HAp) powder from the coral shell in healing critical size mandible gaps in dogs.

Methods: HAp was prepared using the hydrothermal method from coral shells. Characterization of the fabricated coral shell was done by x-ray diffraction (XRD), field emission scanning electron microscopy (FESEM), and energy dispersive x-ray spectroscopy (EDX). The designed research was performed on 18 dogs of both sexes (mean weight: 20±0.5 kg, mean age: 2±0.6 years). The samples were divided into two equal groups. Animals underwent experimental defects at the ventral surface of the lower mandible about 14.5 mm.

Results: The results of XRD represented high crystallinity, the EDX results indicated the surface morphology of distributed particles of calcium, phosphorous, carbon, and oxygen, respectively, and the FESEM results suggested that the surface morphology of HAp appears as a spherical particle that regularly distributed within the sample. In the HAp group, at 30 days, the FESEM images show that the defective gap completely closed, and the center of the defect was filled with a thick layer of osteoid matrix. Radiographically, the HAp group at 30 days post-surgery indicated a well-defined circular radiolucent bone gap at the caudal portion of the mandible, with a partially sclerosed margin. Macroscopically, at 30 days, the gap appears very small and is invaded by new bone formation.

Conclusion: In conclusion, recycling HAp from coral shells has practical value in the reconstitution of the mandibular gap, and the radiological and critical properties of prepared HAp emphasize this outcome.

Keywords: Bone gap, Bone healing, Coral shell, Large size, Mandible

Article info:
Received: 04 July 2023
Accepted: 31 Aug 2023
Publish: 01 Oct 2024

*** Corresponding Author:**
Layth Mahmoud Alkattan, Professor.
Address: *Department of Surgery and Theriogenology, College of Veterinary Medicine, University of Mosul, Mosul, Iraq.*
Phone: *+964 (077) 01631455*
E-mail: *laythalkattan@uomosul.edu.iq*

Introduction

Because of their biochemical properties, availability, simplicity and low fabrication cost, biomaterial bone substitutes are the most used material for reconstructing bone defects (Shafiei-Sarvestani et al., 2012). These materials are commonly used in the orthopedic field as a mandibular defect that comprises the essential affections in maxillofacial bone fracture or discontinuity of the mandible in case of loss of a portion of the lower mandible (Lim et al., 2022). Therefore, the reconstruction of mandibular bone defect poses a real challenge and difficulty for surgeons to the lower jaw's inferior aesthetic point and functional properties (Paré et al., 2019). Hydroxyapatite (HAp) is an inorganic component constituting the bone with the formula $Ca_{10}(PO_4)_6(OH)_2$. It is used as a bone substitute bioactive material due to its osteoconductive biocompatible and nontoxic properties (Szcześ et al., 2017) and used as bone filler. HAp has the same bone composition, is highly biocompatible and stimulates bone growth (Albaroudy et al., 2022; Alkattan et al., 2020). It is inert immunologically and does not provoke sensitive reactions due to the high-heat method used to produce this compound (Cahyaningrum et al., 2018). Recently, bone substitute biomaterials from synthetic or natural sources have been used to treat critical-size bone defects. They have a similar structure to the inorganic bone phase and function as an alternative to metallic grafts and fabricate to make chemical bonds with the bone. They can reconstruct bone defects (Pina et al., 2018; Anvar et al., 2022). Coralline materials and eggshells, considered natural sources of apatite ceramic, can be used as filling materials in orthopedic surgery, in which the chemical structure is closely similar to the inorganic phase of the living bones and teeth (Khan et al., 2019; Zhang et al., 2019). Also, HAp nanoparticles are applied as bone substitute bioactive material that improves the regeneration of the vertical bone model (Kaneko et al., 2020). Many studies suggest that the apatite materials' ionic and mineral elements rapidly incorporate enhanced biocompatibility and provide physicochemical reactions that can accelerate bone formation and regeneration (Atiyah et al., 2021; Pina et al., 2010; Yal Beiranvand et al., 2022). The absence of a well-documented large-size bone gap defect in the dog mandible that was experimentally treated with coral shell HAp powder makes experimental results questionable, so this study suggested determining the effects of prepared coral shell HAp powder in healing of the large-size mandibles bone gap defects in the dog model.

Materials and Methods

The current experimental study used 18 clinically healthy adult local breed dogs of both sexes with a mean weight of 20±0.5 kg and a mean age of 2±0.6 years. All experimental animals were clinically inspected for any infectious disease. All animals were housed at the Animal House of the Veterinary Medicine College, the University of Mosul during the experiment.

Laboratory preparation of coral shell HAp powder

The coral shells (Pectinidae) were purchased from the local market in Basra City, Iraq and then washed using distilled water. Later, the shells were boiled in a mixture of distilled water and ethanol to remove any organic residues. Next, they were dried in an oven at 100 °C for 30 h. The dried shells were grounded to a fine powder using an electrical mortar grinder (Retsch, RM200, China). The powder was calcined in a muffled furnace (Prothrom- Turkey) at 1200 °C for 2 h to produce calcium hydroxide powder. Later, an orthophosphoric acid solution (Ridel- Turkey) with 0.6 M was added to the $Ca(OH)_2$ solution to justify the pH of the solution at 8.5 using a pH meter (AD1000-Germany). The white homogenous precipitate was observed at this point. The product was kept at ambient temperature for 48 hours to age, which allowed the complete chemical reaction. In a muffled furnace, the dried precipitation was calcined at 1200 °C for 2 h. The white crystalline powder was produced (Figure 1), indicating the presence of HAp white crystal powder. Chemical equations are mentioned as Equations 1 (Roudana et al., 2017):

$$CaCo_3 \rightarrow CaO + CO_2 \uparrow$$

$$CaO + H_2O \xrightarrow{\Delta} Ca(OH)_2 + Heat$$

1.

$$10\,Ca(OH)_2 + 6H_3PO_4 \rightarrow$$

$$Ca_{10}(PO_4)_6(OH)_2 + 18H_2O$$

Characterization of fabricated coral shell powder

X-ray diffractometer analysis

The x-ray diffraction (XRD) analyses were performed to determine the crystal phase and purity of the coral shell HAp of samples. The XRD data were recorded within the two theta (2θ) range from 0° to 80° and intensity counts range from 0° to 900° (Malvern Panalytical, Aeris, UK).

Figure 1. Fabricated coral shell hydroxyapatite powder

Field emission scanning electron microscopy (FESEM)

The fabricated coral shell powder's surface morphology, crystal size, and porosity were detected by the FESEM model (INSPECT F 50, FEI, Holland). Also, the FESEM image was taken 30 days after the surgery. All samples were subjected to gold covering before electron microscopy to give the necessary conductivity.

Energy dispersive x-ray spectroscopy (EDX)

The EDX analysis determined the elemental compositions and the relative concentrations of the main trace elements, such as calcium, phosphorous, and oxygen, of the fabricated coral shell HAp powder samples. It is also used to determine the elements distribution mapping to reveal the surface topography of these elements through an energy dispersive x-ray microanalysis system model (INSPECT F 50, FEI, Holland) with an acceleration energy voltage range from 0 to 20 keV. This technique was done in the Ministry of Science and Technology Labs in Baghdad, Iraq (Tatara et al., 2019; Atiyah et al., 2022).

The experimental animals were randomly divided into two equal groups (n=9 in each group):

Group 1: In the control group, a circular mandibular bone gap defect of 14×5 mm in diameter was created in the caudal portion of the mandible using a low-speed bone drill under continuous irrigation with 0.9% sterile saline solution and left empty without any treatment.

Group 2: In the treated group, the same mandibular bone gap defects were created and filled with 5 g of previously fabricated coral shell HAp powder.

Surgical procedure

All operative dogs underwent a protocol of general anesthesia, including a combination of 10% ketamine HCL (Alfasan, Holland) and 2% xylazine (Interchemie, Holland) at a dose of 10 mg/kg and 5 mg/kg, respectively, through intramuscular injection (Greene & Thurmon, 1988; Alkattan & Helal, 2013). The operative region was aseptically prepared, skin incision approximately 4 cm in length was performed along the ventral part of the lower mandible in (the submandibular region) followed by blunt dissection of platysma muscles to expose the mandibular bone (Figure 2A). To create a critical-sized mandibular bone defect in a sagittal incision of approximately 14×5 mm in diameter was made in all groups of the animal, without perforation of the underlying buccal mucosa, using a slow-speed bone drill combined with a diamond hole saw (Juster, j3901, China) with continuous irrigation with 0.9% saline solution to prevent heat damage to the bone tissue to form a circular defect gap (Figure 2B). In the control group, the defective gap was left empty without any treatment in the control group (Figure 2C). The defect gap in the treated group was filled with fabricated coral shell HAp powder (Figure 2D).

Macroscopical evaluations

The site of operation evaluated macroscopically in the control and treated groups 7, 15 and 30 days after the surgery to observe the gross findings within the site of the mandibular bone gap and to inspect any changes.

Radiographical evaluations

The lateral view of the skull was taken immediately after surgery and then at 15, 30 and 60 intervals days post-

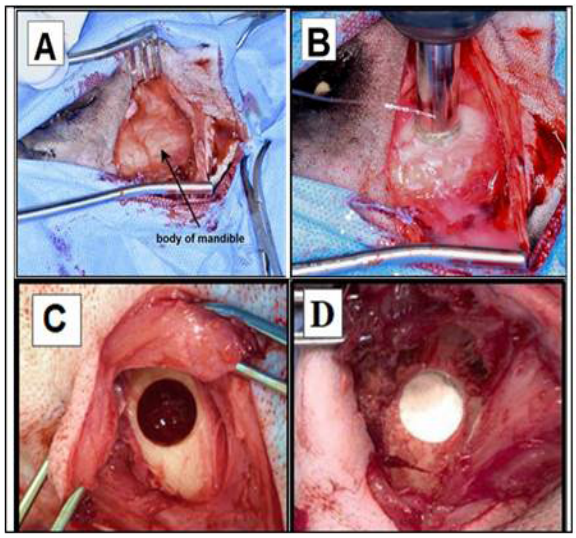

Figure 2. A) Surgical approach to the body of the mandible, B) Creation of circular mandibular bone gap defect, C) The control group, D) The treated group (the defect gap filled with coral shell HAp powder)

surgery, using an x-ray machine (Shimadzu, Japan) accompanied by the digital wireless detector (Italray, Italy) with exposure factors seated as 65 kV and 2.5 mAs, to investigate the position and the density of the bone gap, the presence of periosteal reaction, new bone formation.

Results

Characterization of fabricated coral shell HAp

The results of XRD patterns of the fabricated coral shell HAp powder sample revealed that the typical intense peaks were detected with high crystallinity at 2θ (25.46°, 28.85°, 31.74°, 32.75°, 39.80°, 46.44°, 49.11°, 52.98°, 76.51°), associated with the hexagonal crystalline shape of calcium hydroxide. All these peaks were in agreement with the international center for diffraction data, card number 09-0432 used Qualx software, version 2.25 (Figure 3).

The EDX spectrum of the fabricated coral shell HAp powder, shown in Figure 4, reveals the presence of calcium, phosphorous, oxygen, carbon, and potassium. Quantity values measured in atomic and weight (%) were listed in Table 1. The EDX elemental mapping of fabricated coral shell HAp powder samples shown in Figure 5 was green, blue, purple and yellow, indicating the surface morphology of dispersed calcium, phosphor, carbon and oxygen particles, respectively.

FESEM of coral shell HAp

The surface morphology of the coral shell HAp powder sample heated at 1200 °C for 2 h appears as a spherical particle regularly distributed within the sample with an average diameter of 46.9 µm (Figure 6).

Table 1. The elements content values of the fabricated coral shell HAp powder sample

Elements	%	
	Weight	Atomic
Carbon	13.4	21.5
Oxygen	49.2	59.3
Phosphorous	8.0	5.0
Potassium	10.2	5.0
Calcium	19.2	9.2

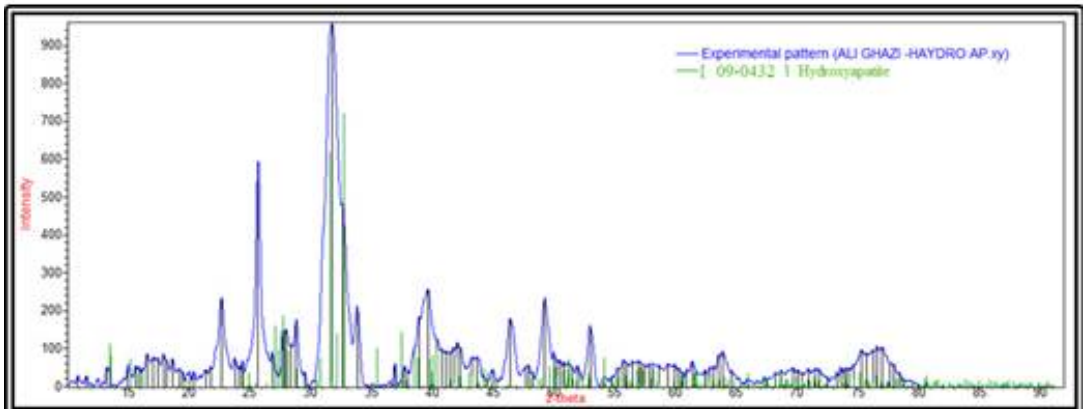

Figure 3. XRD peaks of the fabricated coral shell hap, heated at 1200 ˚C for 2 h, at 2θ range from 0 to 90 degrees and intensity range from 0 to 1000

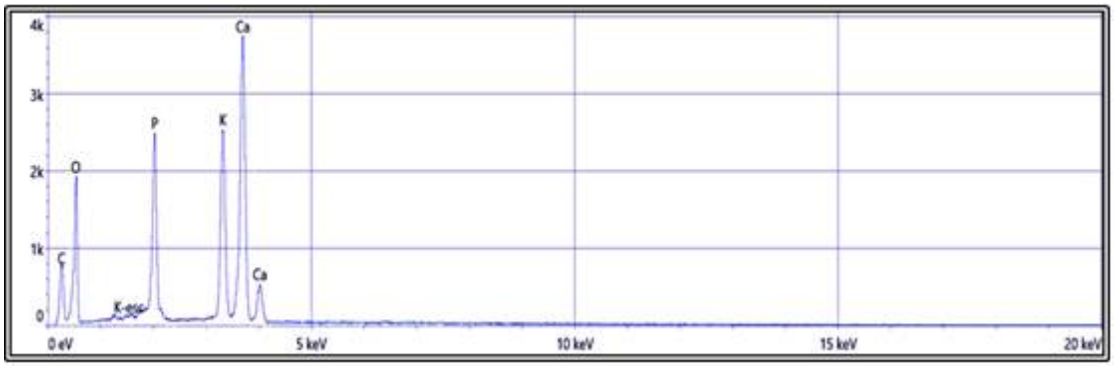

Figure 4. Dispersive EDX elements spectrum analysis of the fabricated coral shell HAp powder

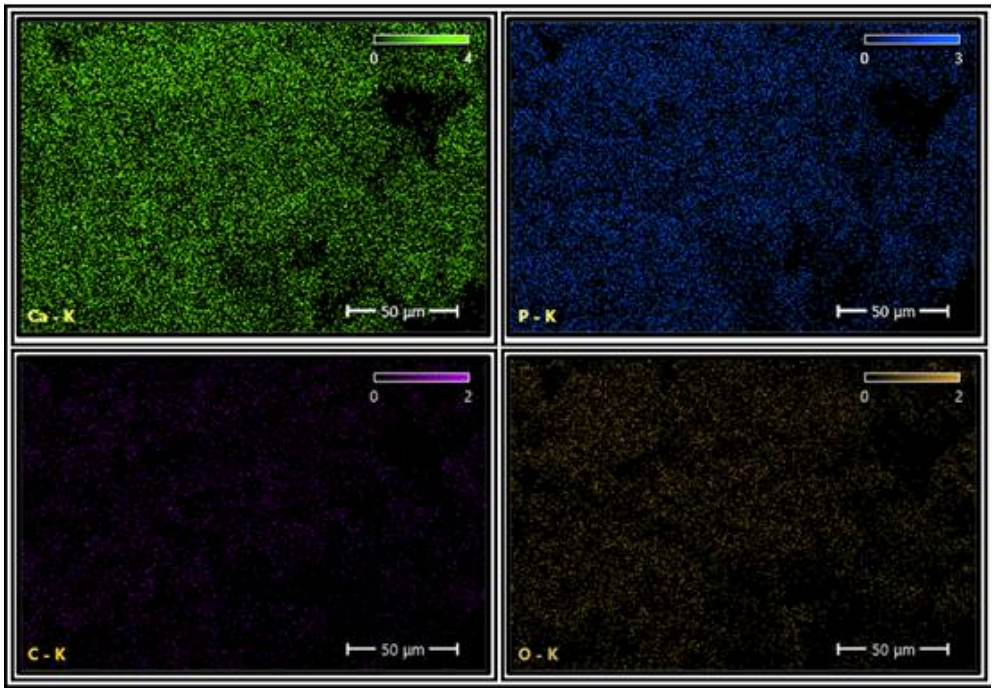

Figure 5. The dispersive EDX elemental mapping analysis of the fabricated coral shell HAp powder sample

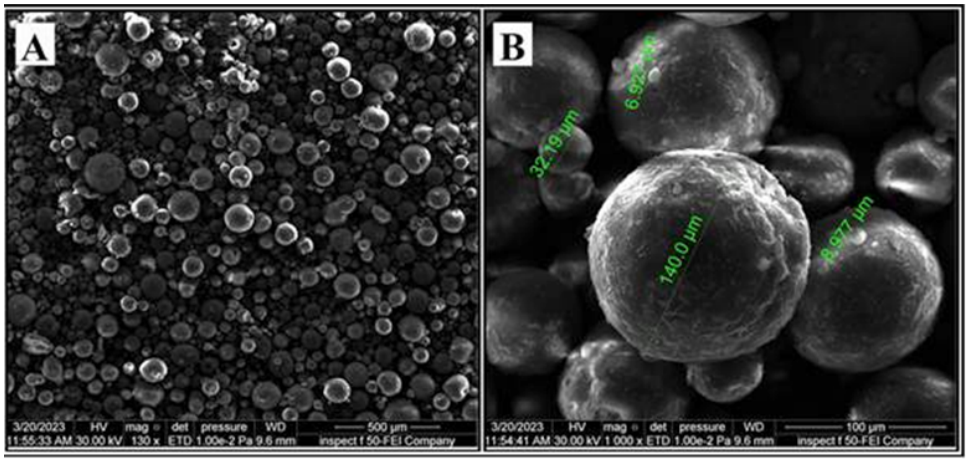

Figure 6. FESEM image of the fabricated coral shell HAp powder obtained at the calcination temperature 1200 ̊C for 2 h

FESEM of the critical size mandibular bone gap defect at 30 days post-surgery

The FESEM images of the defective gap of the mandible bone samples were obtained 30 days post-surgery, as shown in Figure 7. In the control group, the defective gap appeared partially open and the center of the defective gap was filled with a homogenous, smooth matrix surrounded by multiple fibrous tissues, the predominant tissue (Figure 7A).

In the coral shell HAp group, the defective gap appears completely closed and the center of the defect is filled with a thick layer of osteoid matrix, which appears as a light region beyond many lamellar bone excavations that face toward the center of the defective gap (Figure 7B).

Macroscopical results

In the control group, the defective gap seven days post-surgery appears circular without filling tissue. At 15 days post-surgery, excessive fibrous tissue grows within the defective gap. At 30 days post-surgery, the excessive fibrous tissue formation within and around the defective gap, without any signs of calcified or cartilaginous tissue formation, and the size of the defective gap likely appear in the same diameter. While in the HAp group, the defective gap, seven days post-surgery, seemed circular and filled with fibrous tissue. Fifteen days after the surgery, the defective gap appears small in diameter, with a small amount of fibrous tissue within the defective area. At 30 days post-surgery, the defective gap seemed very small in size. The defective gap was slightly filled with a small amount of fibrous tissue, with an invasion of new bone formation from the surrounding bone toward the center of the defective area appears as a firm, solid white mass, and the edges of the defect become rounded, which face inside the center of the defect (Figure 8).

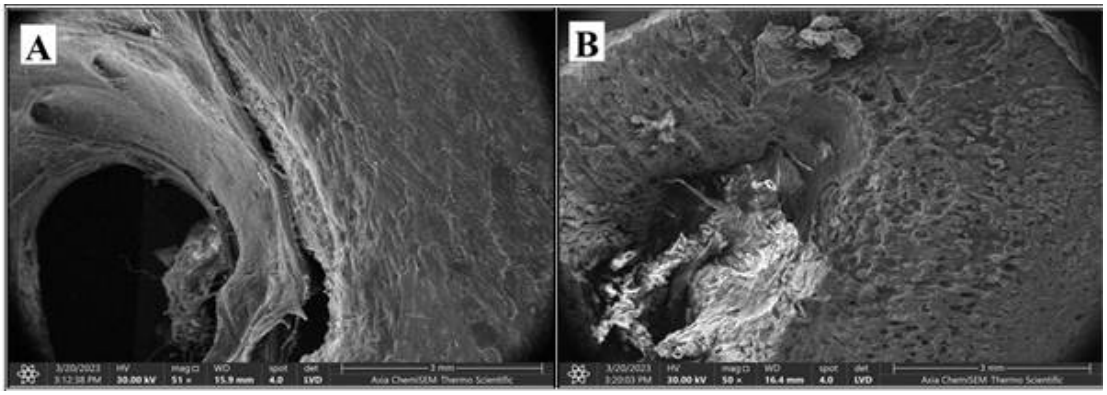

Figure 7. FESEM images of the mandibular bone gap defect at 30 days post-surgery

A) Control group: The defective gap is still open and surrounded by excessive fibrous tissue, B) Coral shell HAp group: The defective gap filled with calcified matrix appears lighter in color and surrounded by lamellar bone

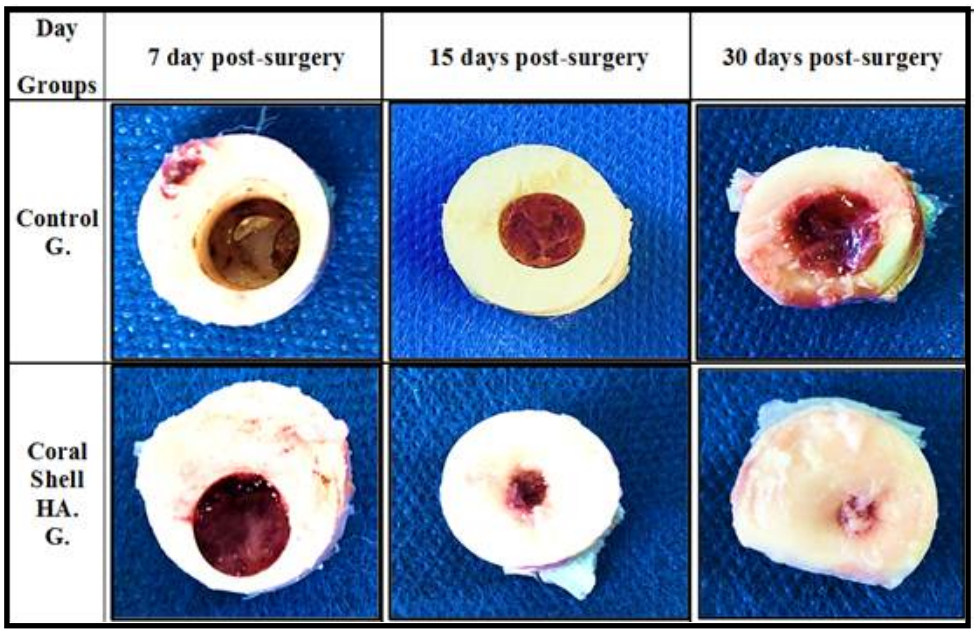

Figure 8. Macroscopical findings of the mandibular bone defect in the control and the treated group at 7, 15 and 30 days after the surgery

Radiographical results

The lateral view of the skull in the control group immediately after the operation represents the induced mandibular bone gap defect which appears as a well-defined circular radiolucent bone defect in the caudal body of the mandible, which seems without trabecular bridging and without any definite significant callus formation, (Figure 9A). At 15 days post-surgery, the radiographic findings in the lateral view of the skull showed a well-defined circular radiolucent bone defect at the caudal portion of the mandible, with a relatively slight increase in density which exhibited in the center of the defective area that represented early little callus formation, but without trabecular bridging (Figure 9B). At 30 days post-surgery, the radiographic finding indicated a well-defined circular radiolucent bone gap defect in the caudal portion of the mandible, with a partially sclerosed margin and a relative increase in the opacity only seen as a very fine area of calcification discarded within the center of the defective gap representing a slight developing callus and without trabecular bridging (Figure 9C). At 60 days post-surgery, the radiographical finding in the lateral view of the skull still appears as a well-defined circular bone defect in the caudal body of the mandible, which remains open and radiolucent, with a partially sclerosed margin. There was a slight increase in the opacity seen as a small area within the center of the defective gap representing the slightly maturing callus without a complete trabecular bridging (Figure 9D).

The radiographical finding in the HAp group immediately after the surgery showed the lateral view of the mandibular bone gap defect, which appears as a well-defined circular radiolucent bone gap defect in the caudal body of the mandible. However, it looks clear with no trabecular bridging or definite significant callus formation (Figure 10A). At 15 days after the operation, the lateral view of the defective gap shows a well-defined, circular, radiolucent bone gap defect in the caudal body of the mandible and there was a relative increase in the opacity seen as haziness throughout the defect representing early callus formation with some trabecular bridging (Figure 10B). At 30 days post-surgery, the defective gap exhibited slightly definite as a circular gap, with a somewhat radiopaque gap defect in the caudal body of the mandible, with a partially sclerosed margin, and there is relatively increased density seen throughout the defect representing developing callus with slightly trabecular bridging (Figure 10C). Lastly, at 60 days after the operation, the radiographical findings show partially-defined semicircular, slightly translucent bone gap defect in the caudal body of the mandible, with a sclerosed margin, and there is a relative increase in density seen in the defect representing the maturing callus with a nearly complete trabecular bridging (Figure 10D).

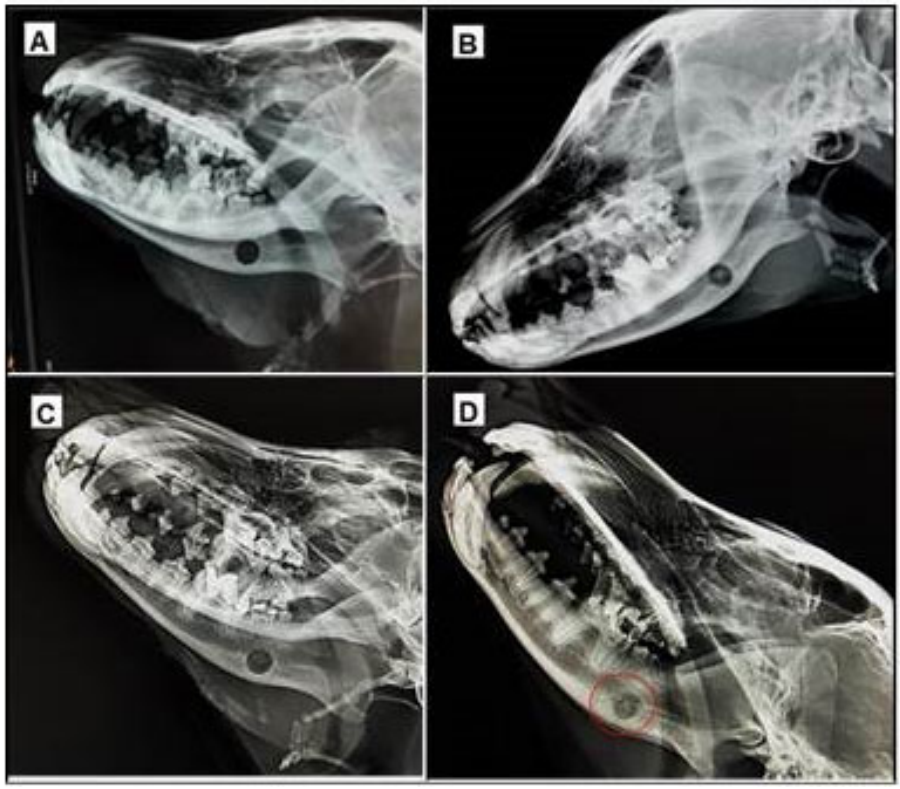

Figure 9. Mandibular bone gap defect in the control group

A) Zero time immediately post-surgery, B) 15 days post-surgery, C) 30 days post-surgery, D) 60 days post-surgery

Figure 10. Mandibular bone gap defect in the HAp group

A) Immediately after the surgery, B) 15 days post-surgery, C) 30 days post-surgery, D) 60 days post-surgery

Discussion

The mandibular bone has several essential functions in the head and neck. It allows mastication by providing a stable counterpoint to the maxilla and as a base for the tooth's attachment. It also facilitates barking, swallowing, and breathing by maintaining space within the oral cavity and allowing the tongue to function.

The FESEM images showed that the coral shell HAp was spherical non-aggregation particles with sizes between 6.9 and 140 µm. The spherical shape of the HAp crystal powder in the coral shell depends on the synthesis method used. It requires prolonged solution rotation using a magnetic stirrer to achieve a reaction with a pH of 8. Thus, this condition results in the slow growth of homogeneously non-agglomerated spherical particles, compared with FESEM images of the quail eggshell $Ca(OH)_2$ which look irregular agglomerated particles due to rapid reaction time that do not require PH justification (Zhou & Lee, 2011). Thus, the FESEM images of fabricated coral shell HAp particles seem more stoichiometric than fabricated quail eggshell $Ca(OH)_2$ particles.

The integration behavior of the analyzed FESEM images of current work at 30 days post-implantation seems to be based on the process of bone tissue regeneration in the HAp group compared to the control group. In this way, the results came in contact with the previous study, which mentioned that the biomaterials might support the directed ingrowth of osteoblasts migrating from the native bone tissue neighbored to the defect site (Barbeck et al., 2020). In contrast, Moshiri et al. (2020) suggested that the shape and the surface morphology are responsible for many of their in vivo biological properties and activities.

Clinically, mandibular bone defects default to reconstitution due to the complex anatomical structure of the jaw and default to soft tissue repair (Tatara et al., 2019). Most defects of the mandible are mainly acquired and rarely congenital causes, which include cysts, benign and malignant tumors, trauma, chronic osteomyelitis, and loss of teeth (Lim et al., 2022). The critical size mandibular bone defect is described as a defect that will not heal spontaneously during the animal's lifetime or using standard treatments (Lim et al., 2022). Dogs have proven to be suitable for studies on the reconstruction of mandibular defects because they easily allow the formation of significant defects with easier surgical access compared to small animals like mice, rats, rabbits and guinea pigs (Huh et al., 2005). Therefore, we evaluated the healing process of the gap defects macroscopically, radiographically, and morphologically with FESEM imaging to determine the critical size of a mandibular gap defect, along with determining the healing effect of coral shell HAp on critically induced mandibular gap defects in dogs.

The results of this study indicated that these bone substitutes are highly biocompatible with the bone tissues because there was no immune rejection or adverse tissue reaction at the defect site. This outcome matches Moshiri et al. (2020) and Mohammed et al. (2023), who mentioned that biomaterials have superior cytocompatibility. Also, Poinern et al. (2014) mentioned that ceramic biomaterials should not induce any cytotoxicity, immunological rejection, or inflammatory responses from the body (Poinern et al., 2014; Roudana et al.,2017; Mohammed et al., 2023). Also, HAp demonstrates an antimicrobial effect, activating new bone tissue formation (Abdul Halim et al., 2021). Thus, it decrees the occurrence of bone tissue infection during the filling of the bone defects with fabricated biomaterials.

Conclusion

We concluded that the fabrication of HAp from natural waste coral shells has practical value in regenerating the mandibular bone gap as a defect in dogs. Future research should investigate the HAp with mesenchymal stem cells to improve the healing process of large-size bone gap defects.

Ethical Considerations

Compliance with ethical guidelines

This study was approved by the Ethics Committee of the University of Mosul, Mosul, Iraq (Code: UM.VET.2022.050).

Funding

This research did not receive any grant from funding agencies in the public, commercial, or non-profit sectors.

Authors' contributions

All authors equally contributed to preparing this article.

Conflict of interest

The authors declared no conflict of interest.

Acknowledgments

The authors are very grateful to the College of Veterinary Medicine, the University of Mosul, Mosul, Iraq, for supporting this study.

References

Abdul Halim, N. A., Hussein, M. Z., & Kandar, M. K. (2021). Nanomaterials-upconverted hydroxyapatite for bone tissue engineering and a platform for drug delivery. *International Journal of Nanomedicine, 16,* 6477-6496. [DOI:10.2147/IJN.S298936] [PMID] [PMCID]

Albaroudy, F. M., Alkattan, L. M., & Ismail, H. K. (2022). Histopathological and serological assessment of using rib lamb xenograft reinforced with and without hydroxyapatite nano gel for reconstruction tibial bone defect in dogs. *Iraqi Journal of Veterinary Sciences, 36*(Supplement1), 69-76. [DOI:10.33899/ijvs.2022.135366.2473]

Alkattan, L., Alawi, A., & Al-Iraqi, O. (2020). The effect of autogenous peritoneal graft augmented with platelets- plasma rich protein on the healing of induced achilles tendon rupture, in dogs. *Iranian Journal of Veterinary Medicine, 14*(2), 111-119. [DOI:10.22059/IJVM.2020.291379.1005037]

Anvar, S. A. A., Nowruzi, B., & Afshari, G. (2023). A review of the application of nanoparticles biosynthesized by microalgae and cyanobacteria in medical and veterinary sciences. *Iranian Journal of Veterinary Medicine, 17*(1), 1-18. [DOI:10.32598/IJVM.17.1.1005309]

Alkattan, L., and Helal, M. (2013).Effects of ketamine-xylazine and propofol-halothane anesthetic protocols on blood gases and some anesthetic parameters in dogs. *Veterinary World, 6*(2), 95-99. [DOI:10.5455/vetworld.2013.95-99]

Atiyah, A. G., Al-Falahi, N. H. R., & Zarraq, G. A. (2021). Synthesis and characterization of porous β-Calcium pyrophosphate bone scaffold derived from avian eggshell. *Pakistan Journal of Zoology, 54*(3), 1439-1442. [DOI:10.17582/journal.pjz/20200730120707]

Barbeck, M., Jung, O., Smeets, R., Gosau, M., Schnettler, R., & Rider, P., et al. (2020). Implantation of an injectable bone substitute material enables integration following the principles of guided bone regeneration. *In Vivo, 34*(2), 557-568. [DOI:10.21873/invivo.11808] [PMID] [PMCID]

Cahyaningrum, S., Herdyastuty, N., Devina, B., & Supangat, D. (2018). Synthesis and characterization of hydroxyapatite powder by wet precipitation method. Paper presented at: International Conference on Chemistry and Material Science (IC2MS) 2017, Malang, East Java, Indonesia, 4–5 November 2017.[DOI:10.1088/1757-899X/299/1/012039]

Greene, S. A., & Thurmon, J. C. (1988). Xylazine-a review of its pharmacology and use in veterinary medicine. *Journal of Veterinary Pharmacology and Therapeutics, 11*(4), 295-313. [DOI:10.1111/j.1365-2885.1988.tb00189.x] [PMID]

Huh, J. Y., Choi, B. H., Kim, B. Y., Lee, S. H., Zhu, S. J., & Jung, J. H. (2005). Critical size defect in the canine mandible. *Oral surgery, Oral Medicine, Oral Pathology, Oral Radiology, and Endodontics, 100*(3), 296–301. [DOI:10.1016/j.tripleo.2004.12.015] [PMID]

Kaneko, A., Marukawa, E., & Harada, H. (2020). Hydroxyapatite nanoparticles as injectable bone substitute material in a vertical bone augmentation model. *In Vivo, 34*(3), 1053-1061. [DOI:10.21873/invivo.11875] [PMID] [PMCID]

Khan, S. R., Jamil, S., Rashid, H., Ali, S., Khan, S. A., & Janjua, M. R. S. A. (2019). Agar and egg shell derived calcium carbonate and calcium hydroxide nanoparticles: Synthesis, characterization and applications. *Chemical Physics Letters, 732,* 136662. [DOI:10.1016/j.cplett.2019.136662]

Lim, H. K., Choi, Y. J., Choi, W. C., Song, I. S., & Lee, U. L. (2022). Reconstruction of maxillofacial bone defects using patient-specific long-lasting titanium implants. *Scientific Reports, 12*(1), 7538. [DOI:10.1038/s41598-022-11200-0] [PMID] [PMCID]

Mohammed, F. M., Alkattan, L. M., Ahmed, M. S., & Thanoon, M. G. (2023). Evaluation the effect of high and low viscosity Nano-hydroxylapatite gel in repairing of an induced critical-size tibial bone defect in dogs: Radiolographical study. *Journal of Applied Veterinary Sciences, 8*(3), 105-110. [DOI:10.21608/javs.2023.215990.1239]

Moshiri, A., Tekyieh Maroof, N., & Mohammad Sharifi, A. (2020). Role of organic and ceramic biomaterials on bone healing and regeneration: An experimental study with significant value in translational tissue engineering and regenerative medicine. *Iranian Journal of Basic Medical Sciences, 23*(11), 1426-1438. [PMID]

Paré, A., Bossard, A., Laure, B., Weiss, P., Gauthier, O., & Corre, P. (2019). Reconstruction of segmental mandibular defects: Current procedures and perspectives. Laryngoscope Investigative Otolaryngology, 4(6), 587-596. [DOI:10.1002/lio2.325] [PMID] [PMCID]

Pina, S., Rebelo, R., Correlo, V. M., Oliveira, J. M., & Reis, R. L. (2018). Bioceramics for osteochondral tissue engineering and regeneration. *Advances in Experimental Medicine and Biology, 1058,* 53–75.[DOI:10.1007/978-3-319-76711-6_3] [PMID]

Pina, S., Vieira, S. I., Rego, P., Torres, P. M., da Cruz e Silva, O. A., & da Cruz e Silva, E. F., et al. (2010). Biological responses of brushite-forming Zn-and ZnSr-substituted beta-tricalcium phosphate bone cements. *European Cells & Materials, 20,* 162–177. [DOI:10.22203/eCM.v020a14] [PMID]

Poinern, G. E., Brundavanam, R. K., Thi Le, X., Nicholls, P. K., Cake, M. A., & Fawcett, D. (2014). The synthesis, characterisation and in vivo study of a bioceramic for potential tissue regeneration applications. *Scientific Reports, 4*(1), 6235. [DOI:10.1038/srep06235] [PMID] [PMCID]

Shafiei-Sarvestani, Z., Oryan, A., Bigham, A. S., & Meimandi-Parizi, A. (2012). The effect of hydroxyapatite-hPRP, and coral-hPRP on bone healing in rabbits: Radiological, biomechanical, macroscopic and histopathologic evaluation. *International Journal of Surgery (London, England), 10*(2), 96–101. [DOI:10.1016/j.ijsu.2011.12.010] [PMID]

Roudana, M. A., Ramesha, S., Niakanb, A., Wonga, Y. H., Zavareha, M. A., & Chandranc, H, et al. (2017). Thermal phase stability and properties of hydroxyapatite derived from biowaste eggshells. *Journal of Ceramic Processing Research, 18*(1), 69-72. [Link]

Szcześ, A., Hołysz, L., & Chibowski, E. (2017). Synthesis of hydroxyapatite for biomedical applications. *Advances in Colloid and Interface Science, 249,* 321-330. [DOI:10.1016/j.cis.2017.04.007] [PMID]

Tatara, A. M., Koons, G. L., Watson, E., Piepergerdes, T. C., Shah, S. R., & Smith, B. T., et al. (2019). Biomaterials-aided mandibular reconstruction using in vivo bioreactors. *Proceedings of the National Academy of Sciences of the United States of America, 116*(14), 6954–6963. [DOI:10.1073/pnas.1819246116] [PMID] [PMCID]

Yal Beiranvand, S., Nourani, H., & Kazemi Mehrjerdi, H. (2022). Fabrication of platelet-rich fibrin-coated polycaprolactone/hydroxyapatite (PCL-HA/PRF) 3D printed scaffolds for bone tissue engineering. *Iranian Journal of Veterinary Medicine, 16*(4), 400-413. [DOI:10.22059/IJVM.2022.335899.1005219]

Zhang, H., Zhou, Y., Yu, N., Ma, H., Wang, K., & Liu, J., et al. (2019). Construction of vascularized tissue-engineered bone with polylysine-modified coral hydroxyapatite and a double cell-sheet complex to repair a large radius bone defect in rabbits. *Acta Biomaterialia, 91,* 82–98. [DOI:10.1016/j.actbio.2019.04.024] [PMID]

Zhou, H., & Lee, J. (2011). Nanoscale hydroxyapatite particles for bone tissue engineering. *Acta Biomaterialia, 7*(7), 2769-2781. [DOI:10.1016/j.actbio.2011.03.019] [PMID]

This Page Intentionally Left Blank